

## Tailoring the phonon band structure in binary colloidal mixtures

Julia Fornleitner,<sup>1,2</sup> Gerhard Kahl,<sup>1</sup> and Christos N. Likos<sup>3,4</sup>

<sup>1</sup>Center for Computational Materials Science and Institut für Theoretische Physik,  
Technische Universität Wien, Wiedner Hauptstraße 8-10, A-1040 Vienna, Austria

<sup>2</sup>Institut für Festkörperforschung–Theorie II, Forschungszentrum Jülich, D-52425 Jülich, Germany

<sup>3</sup>Institute of Theoretical Physics, Heinrich-Heine University of Düsseldorf, D-40225 Düsseldorf, Germany

<sup>4</sup>Faculty of Physics, University of Vienna, Boltzmannstraße 5, A-1090 Vienna, Austria

(Received 22 February 2010; published 22 June 2010)

We analyze the phonon spectra of periodic structures formed by two-dimensional mixtures of dipolar colloidal particles. These mixtures display an enormous variety of complex ordered configurations [J. Fornleitner *et al.*, *Soft Matter* **4**, 480 (2008)], allowing for the systematic investigation of the ensuing phonon spectra and the control of phononic gaps. We show how the shape of the phonon bands and the number and width of the phonon gaps can be controlled by changing the susceptibility ratio, the composition, and the mass ratio between the two components.

DOI: [10.1103/PhysRevE.81.060401](https://doi.org/10.1103/PhysRevE.81.060401)

PACS number(s): 82.70.Dd, 63.22.-m

Materials with a band gap in their spectrum of transmitted sound waves have been the focus of intensive research recently. Most often, these “phononic crystals,” termed in analogy to the more familiar photonic crystals, are analyzed and fabricated on the basis of macroscopic approaches: following methods from scattering theory, materials with a periodic modulation in their elastic properties and/or density are assembled, so that mismatches in the speed of sound and destructive interference lead to the desired gaps [1–4]. Instead of treating the whole system as a continuous medium with periodically modulated elastic moduli, we employ a microscopic approach based on interparticle interactions, which directly determine the particle motions. The latter uniquely determine *both* the ground-state configuration of the system *and* its elementary excitations above the same, i.e., the phonons. A class of materials where this microscopic approach is particularly fruitful are colloidal crystals. In such systems, the interactions are tunable and versatile. It has been shown that the dispersion curves of two-dimensional colloidal crystals can be shaped and controlled by suitable external substrate potentials [5–7]. Here, we focus on systems that exhibit phononic gaps without the presence of external fields, namely, *mixtures*: the nontrivial unit cells of their ground states give rise to optical branches in the phonon band structure (PBS), thus, opening the possibility to induce gaps by suitable adjustments in the interactions. Here, we explore the possibilities to tune the PBS’s of a binary mixture of dipolar colloids via changes in the susceptibility ratio and composition.

Binary dipolar monolayers are readily available to experiments [8–13] and exhibit a rich wealth of stable ordered structures [14,15]. Experimental realizations employ superparamagnetic particles of different susceptibilities  $\chi$ , which are trapped at the interface of a pendant water droplet to ensure a planar geometry [13]. An external magnetic field  $\mathbf{B}$  applied perpendicular to the water-air-interface induces magnetic moments in the colloidal particles parallel to the external field,  $\mathbf{M}_i = \chi_i \mathbf{B}$ , with  $i = A, B$  labeling the particle species. We emphasize that here the external field serves only as a means to influence the *two-body interactions* in the Hamiltonian and does not act on the systems as a *one-body poten-*

*tial*, as is the case of laser beams in Refs. [5–7]. Thus, the structures form naturally in the system by means of self-assembly. For the sake of simplicity, we assume that the physical size of the two-particle species is the same and given by their common diameter  $\sigma$ , the disparity in their interactions arising from different degrees of doping with ferromagnetic material, such as  $\text{Fe}_2\text{O}_3$ . Setting  $m_i = \chi_i / \chi_A \leq 1$ , the ideal dipole-dipole repulsion acting in the mixture can be written as  $\Phi_{ij}(x) = \varepsilon m_i m_j / x^3$ ,  $i, j = A, B$ , with  $x = r / \sigma$  and  $\varepsilon = \mu_0 \chi_A^2 |\mathbf{B}|^2 / (4\pi\sigma^3)$ . The ground state is, thus, determined by the asymmetry in dipole strength, given by  $m = \chi_B / \chi_A < 1$ , and by the composition of the mixture,  $C = n_B / (n_A + n_B)$ , with  $n_{A(B)}$  being the number of strong (weak) dipoles per unit cell.

Colloids in solution obey Langevin dynamics and their full equations of motion include the interparticle forces, the random collisions with the solvent and hydrodynamic interactions [16], involving the masses of the particles, the frictions constants and the solvent properties via the Navier-Stokes equations. Accordingly, the full dynamics of colloidal crystals have been thoroughly analyzed by theory and experiment in the past [16–19]. Here, we focus only on the excitation spectrum of the crystal, which is expressed in terms of the dispersion relation  $\lambda(\mathbf{q})$ , where  $\mathbf{q}$  denotes a wave vector in the first Brillouin zone. Although oscillations in a colloidal crystal are overdamped, the quantities  $\lambda(\mathbf{q})$  are still experimentally measurable by means of the equipartition theorem [5], a strategy that has been successfully applied to the one-component version of the system at hand [11].

Accordingly, we apply harmonic lattice theory [20,21] and obtain the dispersion curves  $\lambda(\mathbf{q})$  by solving the eigenvalue equation  $\lambda(\mathbf{q}) c_{\nu i} = \sum_{\nu' i'} \tilde{D}_{\nu i, \nu' i'}(\mathbf{q}) c_{\nu' i'}$ , where  $\tilde{D}_{\nu i, \nu' i'}(\mathbf{q})$  is the Fourier transform of the dynamical matrix  $D_{\nu i, \nu' i'}(n, n')$ , defined as:

$$D_{\nu i, \nu' i'}(n, n') = \frac{\partial^2 \Phi(\mathbf{r}^N)}{\partial u_{n\nu i} \partial u_{n' \nu' i'}} \Big|_{\mathbf{u}^N = 0}. \quad (1)$$

Here, the index  $n$  is used to label the unit cell in the lattice and  $\nu$  runs over all particles within one unit cell,

$\nu=1, \dots, n_A+n_B$ , with  $\mathbf{u}_{n\nu}$  being the displacement of the  $\nu$ th particle in the  $n$ th unit cell of the lattice from its equilibrium position. Finally, the index  $i$  denotes the Cartesian components,  $i=x, y$ , and  $\Phi(\mathbf{r}^N)$  is the total potential energy of the crystal at the harmonic approximation. The dimensionless eigenvalues  $\lambda(\mathbf{q})\sigma^2/\varepsilon$  are determined for  $\mathbf{q}$  values along those axes of the first Brillouin zone that link the points of high symmetry within the same. For the case of Newtonian dynamics, and for typical values of  $\mathbf{B}$  and colloidal properties [13], the  $\lambda(\mathbf{q})$  (and the associated gaps) correspond to frequencies of 1–50 kHz.

In addition to affecting the ground states, the susceptibility ratio  $m$  can be used to fine-tune the appearance of a PBS corresponding to a given ground state, as the stable configurations are robust against small variations in  $m$ . In the following discussion, we focus on mixtures with  $C \geq 1/2$ , as the complexity in the emerging patterns increases with the number of weak dipoles in the system and the PBS's reflect recurrences in the ground states.

We start by demonstrating the influence of the susceptibility ratio  $m$  on the PBS for mixtures with a composition of  $C=1/2$ . We vary the susceptibility ratio in a range from  $m=0.003$  to  $m=0.41$  and calculate the PBS's for the ground states predicted in Refs. [14,15]. In Fig. 1, we show the phonon spectra for  $C=1/2$  and increasing susceptibility ratio from top to bottom ( $m=0.018, 0.04, 0.18$ , and  $0.41$ ). The corresponding ground states, together with their first Brillouin zones and the path along which the PBS's were determined, are depicted in Fig. 1 as well. At the chosen composition, the dipolar mixture develops three different types of ground states depending on  $m$ . For very low  $m$  values, the stronger dipoles form a hexagonal lattice unaffected by the presence of the weaker species, the latter arranging themselves in lanes and occupying interstitial sites. The associated PBS is characterized by a nonuniform distribution of dispersion curves: the topmost four branches span a much broader eigenvalue range than the remaining four modes at the bottom of the band structure. In addition, the “unfurled” upper branches are separated from the compressed lower region by a distinctive gap, see Fig. 1(a). Small increases in the susceptibility ratio  $m$  leave the ground state unchanged, despite of the fact that interactions involving the weaker species intensify [14,15]. In the PBS, a small increase in  $m$  is reflected by a widening of the gap and a gradual expansion of the lower dispersion curves. Above a certain threshold in  $m$ , the weak dipoles are able to distort the hexagonal pattern of their stronger counterparts. This decrease in symmetry in the ground state is also reflected in the PBS, see Fig. 1(b). At susceptibility ratios between  $m=0.06$  and  $0.18$ , a regular square lattice is predicted to be the energetically most favorable arrangement of dipoles [15]. In the PBS's associated to the quadratic configuration, the four dispersion curves cover the eigenvalue range in a uniform fashion: all branches are fully unfurled and no gaps occur. Variations in the susceptibility ratio that leave the ground-state unchanged result in a stretching of the PBS without altering its general appearance. As an example, Fig. 1(c) shows the PBS of the square lattice formed at  $m=0.18$ . For  $m \geq 0.28$ , the ground state of the binary mixture changes from the regular square lattice to the  $H_2$  structure [22], which consists of distorted hexagons of

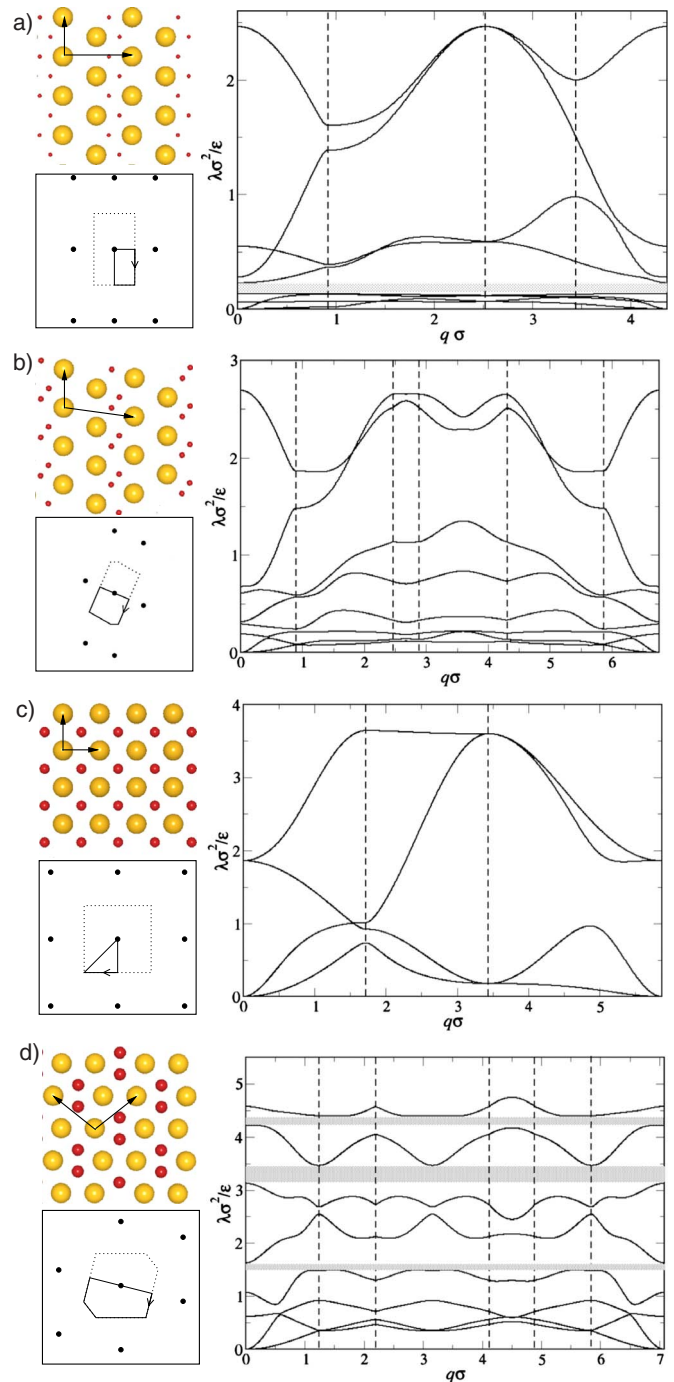


FIG. 1. (Color online) Phonon band structures for a binary mixture of dipolar colloids with a composition of  $C=1/2$  and susceptibility ratios of (a)  $m=0.018$ , (b)  $m=0.04$ , (c)  $m=0.18$ , and (d)  $m=0.28$ . Band gaps are marked by shaded regions; dashed vertical lines mark the corners of the reduced path of  $\mathbf{q}$  values. The corresponding ground-state is depicted on the top left of each band structure, with the species of stronger (weaker) dipoles given by yellow (red) spheres and two lattice vectors marking the chosen unit cell. The sphere size reflects the dipole strength. On the bottom left of each band structure, a cell of the reciprocal lattice with its first Brillouin zone, marked by broken lines, is shown. The path of  $\mathbf{q}$  values along which the band structures were determined, is indicated by a full line.

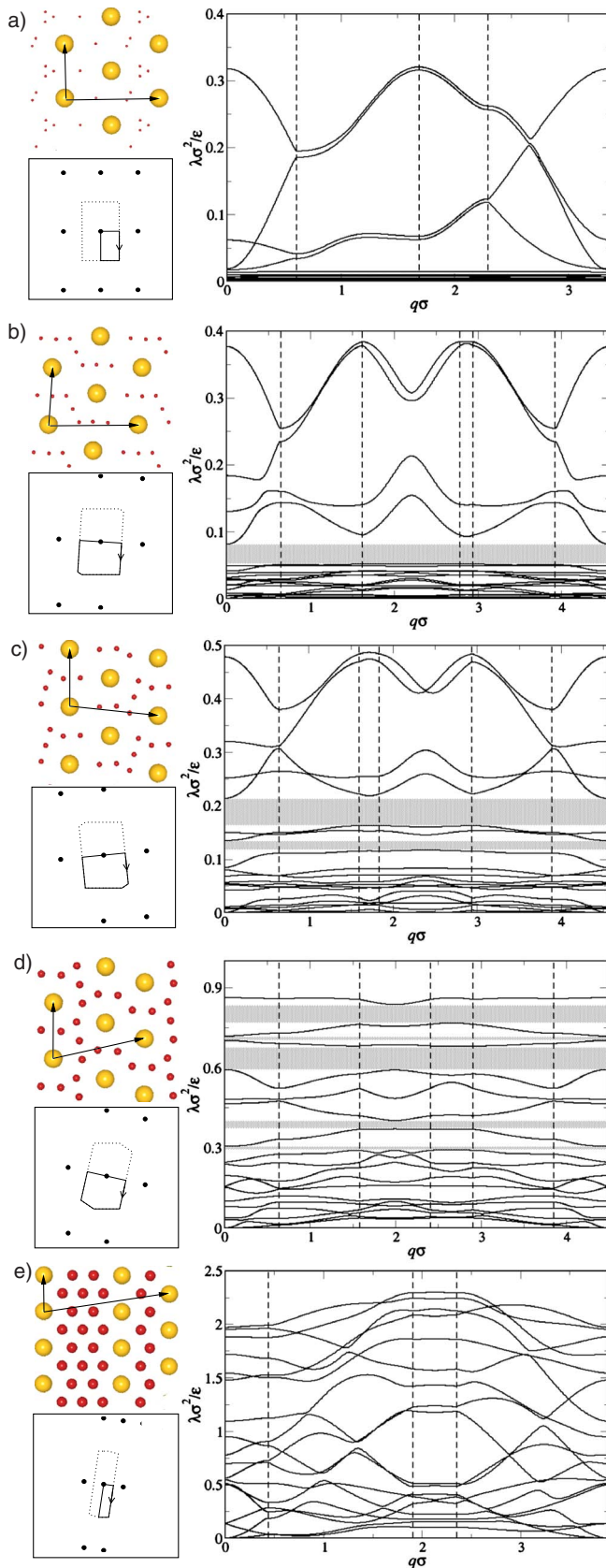


FIG. 2. (Color online) Phonon band structures for a binary mixture of dipolar colloids with a composition of  $C=7/9$  and susceptibility ratios of (a)  $m=0.003$ , (b)  $m=0.018$ , (c)  $m=0.04$ , (d)  $m=0.09$ , and (e)  $m=0.28$ .

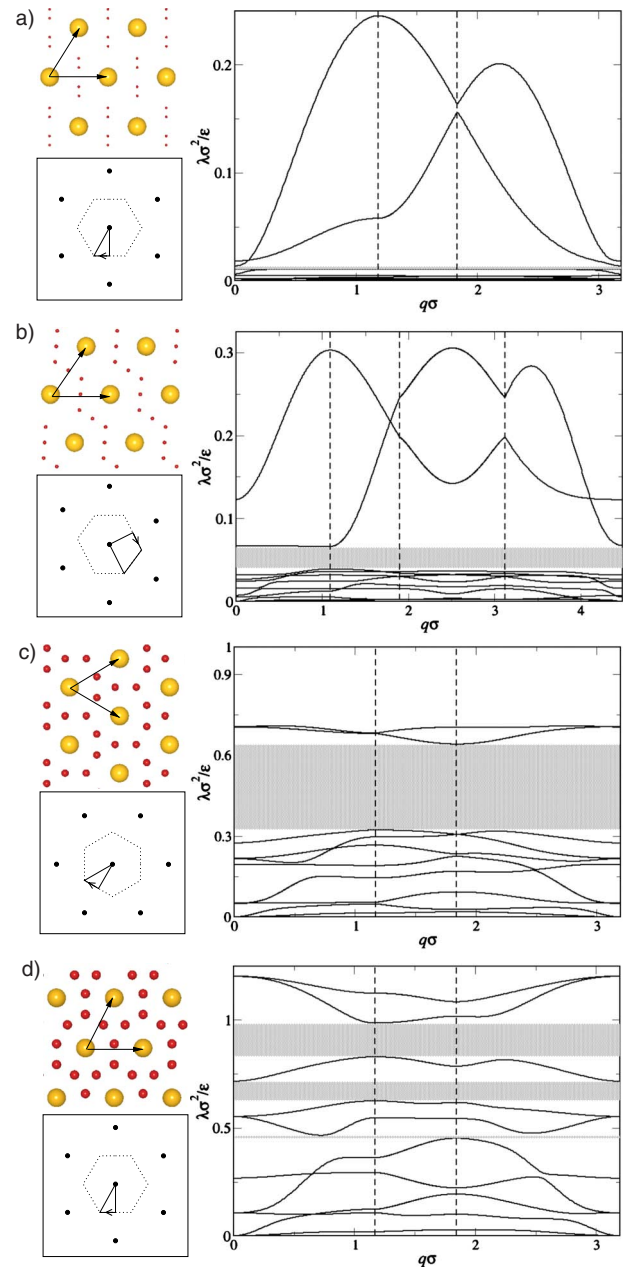


FIG. 3. (Color online) Phonon band structures for a binary mixture of dipolar colloids with a composition of  $C=4/5$  and  $m$  values: (a)  $m=0.003$ , (b)  $m=0.018$ , (c)  $m=0.09$ , (d)  $m=0.18$ .

strong dipoles accommodating two particles of the weaker species. The PBS's of the  $H_2$  lattice are again characterized by the occurrence of distinct eigenvalue bands. The number of these bands and the width of the gaps separating them from each other are tunable via the susceptibility ratio: at  $m=0.28$ , i.e., close to the transition from the square to the  $H_2$  lattice, three gaps are observed, see Fig. 1(d).

At higher concentrations of weak dipoles, more exotic particle arrangements with a low degree of symmetry appear among the ground states. For the PBS's, the trends described above become more pronounced. In Fig. 2 we show selected PBS's obtained for mixtures with  $C=7/9$  and susceptibility ratios in the range from  $m=0.003$  to  $m=0.28$ . At small values of  $m$ , the non-uniform distribution of dispersion curves is

recovered. The four curves at the top of the PBS again cover a much broader eigenvalue range than the rest of the branches and a gap separating the compact from the extended dispersion curves is observed, even at very low values of  $m$ . The susceptibility ratio can again be used to tune the gap width, see Figs. 2(a) and 2(b). In contrast to the previous case,  $C=1/2$ , the distortion of the underlying hexagonal lattice induced by an increase of  $m$ , does not destroy the separation of the PBS into distinct bands. A further increase in  $m$  opens, on the contrary, additional gaps, first, by causing branches from the lower, compressed region to detach and then, with the pattern of weak dipoles approaching a circular arrangement, by a progressive flattening of the topmost curves, as the  $\lambda(\mathbf{q})$  decreasingly depend on the direction of propagation in the crystal [see Figs. 2(c) and 2(d)]. At  $m=0.09$ , Fig. 2(d), a maximum of five distinct bands is reached. If the susceptibility ratio is increased above a certain threshold, i.e.,  $m \geq 0.18$ , the ground state of the mixture undergoes a transition to lane-like arrangements. This change forces all gaps to close and leads to a uniform distribution of well modulated dispersion curves, see Fig. 2(e), reflecting the growing similarity of the two species and mirroring the dominant hexagonal structure of the crystal.

The general trends become even clearer in the sequence of PBS's obtained at  $C=4/5$ , see Fig. 3, for PBS calculated at  $m=0.003, 0.018, 0.09$ , and  $0.18$ . The band structures at low values of  $m$  are characterized by two distinct bands, the width of the gap separating them is well tunable via the susceptibility ratio, Figs. 3(a) and 3(b). At intermediate values of  $m$ , the dispersion curves flatten out and multiple gaps appear between the less modulated branches, see Figs. 3(c) and 3(d), which vanish again with the onset of lane formation observed at high-susceptibility ratios.

Thus far, we have not considered a possible mass asymmetry of the two species in our calculations. This is done because the colloidal systems that allow for an experimental

realization of our findings are mostly *Brownian systems*, in which the mass of the particles is rendered irrelevant by overdamping [5,11]. Nevertheless, an experimental setup in which the colloidal particles are confined between two parallel plates is readily available [23], and evaporation of the solvent from the cell would lead to Newtonian dynamics for the colloids. Including the particle masses  $M_v$  by multiplying expression Eq. (1) for the dynamical matrix with  $1/\sqrt{M_v M_{v'}}$ , we can easily switch to *Newtonian systems* in our theoretical approach and gain the mass ratio  $M=M_B/M_A$  as an additional parameter to tune the PBS's with. In ongoing investigations we have found that mass asymmetry (as it occurs, for instance, in dusty plasmas) enhances the effects described above: by lowering  $M$ , the topmost  $2n_A$  branches can be decoupled from the rest of the band structure and shifted to higher eigenvalues, thus opening a gap of variable width. In addition, the flattening of dispersion curves gets more pronounced with increasing mass-asymmetry, so that even completely flat branches can be induced on the PBS's.

In summary, we have investigated the possibility to control the PBS's of a dipolar binary mixture via the parameters determining the interactions and the ground state of the system. By calculation of the dispersion curves for the stable particle arrangements, we could show that, for systems with a majority of weaker dipoles, multiple gaps can be opened by suitable adjustments in the susceptibility ratio  $m$ . In addition, remarkably flat branches were observed in the PBS featuring multiple gaps. Our results are easily verifiable in experimental setups that employ two-dimensional binary magnetic colloids, where dispersion curves can be measured by means of the equipartition theorem [5,11].

We thank P. Keim and S. U. Egelhaaf for helpful discussions. This work has been supported by the FWF under Project No. P17823 and by the SFB-TR6, Project C3.

- 
- [1] R. S. Penciu *et al.*, *EPL* **58**, 699 (2002).  
 [2] W. Cheng *et al.*, *Nature Mater.* **5**, 830 (2006).  
 [3] T. Still *et al.*, *Phys. Rev. Lett.* **100**, 194301 (2008).  
 [4] J.-F. Robillard *et al.*, *Appl. Phys. Lett.* **95**, 124104 (2009).  
 [5] H. H. von Grünberg and J. Baumgartl, *Phys. Rev. E* **75**, 051406 (2007).  
 [6] J. Baumgartl, M. Zvyagolskaya, and C. Bechinger, *Phys. Rev. Lett.* **99**, 205503 (2007).  
 [7] J. Baumgartl *et al.*, *Soft Matter* **4**, 2199 (2008).  
 [8] K. Zahn, R. Lenke, and G. Maret, *Phys. Rev. Lett.* **82**, 2721 (1999).  
 [9] K. Zahn and G. Maret, *Phys. Rev. Lett.* **85**, 3656 (2000).  
 [10] K. Zahn, A. Wille, G. Maret, S. Sengupta, and P. Nielaba, *Phys. Rev. Lett.* **90**, 155506 (2003).  
 [11] P. Keim, G. Maret, U. Herz, and H. H. von Grünberg, *Phys. Rev. Lett.* **92**, 215504 (2004).  
 [12] N. Hoffmann, F. Ebert, C. N. Likos, H. Löwen, and G. Maret, *Phys. Rev. Lett.* **97**, 078301 (2006).  
 [13] F. Ebert, P. Keim, and G. Maret, *Eur. Phys. J. E* **26**, 161 (2008).  
 [14] J. Fornleitner *et al.*, *Soft Matter* **4**, 480 (2008).  
 [15] J. Fornleitner *et al.*, *Langmuir* **25**, 7836 (2009).  
 [16] A. J. Hurd, N. A. Clark, R. C. Mockler, and W. J. O'Sullivan, *Phys. Rev. A* **26**, 2869 (1982).  
 [17] J. Derksen and W. van de Water, *Phys. Rev. A* **45**, 5660 (1992).  
 [18] Y. N. Ohshima and I. Nishio, *J. Chem. Phys.* **114**, 8649 (2001).  
 [19] R. Piazza and V. Degiorgio, *Phys. Rev. Lett.* **67**, 3868 (1991).  
 [20] N. W. Ashcroft and N. D. Mermin, *Solid State Physics* (Saunders College, Fort Worth, 1976).  
 [21] M. Marder, *Condensed Matter Physics* (Wiley, New York, 2000).  
 [22] C. N. Likos and C. L. Henley, *Philos. Mag. B* **68**, 85 (1993).  
 [23] N. Osterman, D. Babic, I. Poberaj, J. Dobnikar, and P. Zihlerl, *Phys. Rev. Lett.* **99**, 248301 (2007).